DOI: 10.1002/chem.201202499

A Biomimetic Pathway for Vanadium-Catalyzed Aerobic Oxidation of Alcohols: Evidence for a Base-Assisted Dehydrogenation Mechanism

Bethany N. Wigington,[a] Michael L. Drummond,[b] Thomas R. Cundari,*[b] David L. Thorn,[c] Susan K. Hanson,*[c] and Susannah L. Scott*[a, d]

Abstract: The first step in the catalytic oxidation of alcohols by molecular O_2, mediated by homogeneous vanadium(V) complexes $[LV^V(O)(OR)]$, is ligand exchange. The unusual mechanism of the subsequent intramolecular oxidation of benzyl alcoholate ligands in the 8-hydroxyquinolinato (HQ) complexes $[(HQ)_2V^V(O)(OCH_2C_6H_4\text{-}p\text{-}X)]$ involves intermolecular deprotonation. In the presence of triethylamine, complex **3** (X = H) reacts within an hour at room temperature to generate, quantitatively, $[(HQ)_2V^{IV}(O)]$, benzaldehyde (0.5 equivalents), and benzyl alcohol (0.5 equivalents). The base plays a key role in the reaction: in its absence, less than 12% conversion was observed after 72 hours. The reaction is first order in both **3** and NEt_3, with activation parameters $\Delta H^{\ddagger} = (28 \pm 4)\ kJ\,mol^{-1}$ and $\Delta S^{\ddagger} = (-169 \pm 4)\ J\,K^{-1}\,mol^{-1}$. A large kinetic isotope effect, 10.2 ± 0.6, was observed when the benzylic hydrogen atoms were replaced by deuterium atoms. The effect of the *para* substituent of the benzyl alcoholate ligand on the reaction rate was investigated using a Hammett plot, which was constructed using σ_p. From the slope of the Hammett plot, $\rho = +(1.34 \pm 0.18)$, a significant buildup of negative charge on the benzylic carbon atom in the transition state is inferred. These experimental findings, in combination with computational studies, support an unusual bimolecular pathway for the intramolecular redox reaction, in which the rate-limiting step is deprotonation at the benzylic position. This mechanism, that is, base-assisted dehydrogenation (BAD), represents a biomimetic pathway for transition-metal-mediated alcohol oxidations, differing from the previously identified hydride-transfer and radical pathways. It suggests a new way to enhance the activity and selectivity of vanadium catalysts in a wide range of redox reactions, through control of the outer coordination sphere.

Keywords: aerobic oxidation · base-assisted catalysis · biomimetic synthesis · Hammett correlation · vanadium

Introduction

The development of selective aerobic oxidation catalysts is desirable for the production of many important fine chemical products.[1] Dioxygen has significant advantages over stoichiometric metal-based oxidants and even organic oxidants; these advantages include low cost, ready availability, low toxicity, and an environmentally benign reaction byproduct (H_2O). Complexes of several noble transition metals, including Pd,[2] Rh,[3] and Ru,[4] have proven to be versatile catalysts in a wide range of aerobic oxidation reactions. There is also strong interest in the design of oxidation catalysts based on Earth-abundant metals, such as V[5] and Cu.[6] However, these catalysts typically operate by redox mechanisms that are very different from those of the noble metals, the former showing greater propensity to engage in one-electron (radical) processes.[7] Hence, an important factor in "reverse engineering" noble-metal catalysts using base metals as their replacements is the potential selectivity issues arising from radical chemistry.[8] In this context, it is interesting that Nature uses 3d metals, such as Fe and Cu, to oxidize even the most inert C–H bonds selectively.[9] Metalloenzymes are adept at using both inner and outer coordination sphere interactions for controlling activity and selectivity. Nevertheless, most biomimetic approaches, with some notable recent exceptions,[10] have emphasized inner coordination sphere chemistry.[11] Methods of inducing two-electron reactivity, long a hallmark of the 4d and 5d metals, through the participation of noncoordinated sites may be the key to a greater exploitation of 3d metals in catalysis.[12]

In view of these criteria, the rational design of environmentally benign oxidation catalysts requires a detailed un-

[a] B. N. Wigington, Prof. Dr. S. L. Scott
Department of Chemistry and Biochemistry
University of California, Santa Barbara, CA 93106-9510 (USA)

[b] Dr. M. L. Drummond, Prof. Dr. T. R. Cundari
Department of Chemistry
Center for Advanced Scientific Computing and Modeling (CASCaM)
University of North Texas, Denton, TX 76201 (USA)
E-mail: thomas.cundari@unt.edu

[c] Dr. D. L. Thorn, Dr. S. K. Hanson
Chemistry Division
Los Alamos National Laboratory
Los Alamos, New Mexico 87545 (USA)
E-mail: skhanson@lanl.gov

[d] Prof. Dr. S. L. Scott
Department of Chemical Engineering
University of California, Santa Barbara 93106-5080 (USA)
Fax: (+1) 805-893-4731
E-mail: sscott@engineering.ucsb.edu

Supporting information for this article is available on the WWW under http://dx.doi.org/10.1002/chem.201202499.

derstanding of the mechanisms of transition-metal-mediated oxidations. This is illustrated in the recent development of Pd-based systems for aerobic alcohol oxidation, for which mechanistic insight into the role of ligand modulation and base promoters led to the design of robust, active, and selective catalysts.[2a,d,e]

Aerobic oxidation using vanadium catalysts may have an even wider substrate scope and application. Mild and selective vanadium-catalyzed oxidation reactions of benzylic, allylic, and propargylic alcohols has been demonstrated.[13] Vanadium/Schiff base complexes are highly enantioselective catalysts for the aerobic oxidative kinetic resolution of α-hydroxy-esters, -amides, and -phosphonates at ambient temperature.[14] Vanadium complexes induce oxidative decarboxylation in certain hydroxy carboxylic acids[15] and α-amino acids,[16] desilylation of benzylic silanes,[17] as well as oxidation of lignin model compounds.[18] However, the mechanisms of vanadium-mediated oxidation reactions are comparatively less well understood.

The facile interconversion of vanadium oxidation states (for example, V^{V}, V^{IV}, and V^{III}) can make it difficult to identify redox pathways. In alcohol oxidations, both hydrogen atom abstraction[5e,19] and hydride abstraction[5c,d,f,14b,c,18] by the vanadyl oxo ligand have been postulated. Littler and Waters proposed the former, based on indirect evidence of radical intermediates and the appearance of C−C bond-fission products.[20] Similarly, Roček and Aylward reported that VO_2^+ reacts with 2-ethyl-cyclobutanol by a radical pathway to give the ring-opened product, 4-hydroxyhexanal.[19] In other cases, the absence of ring-scission products has been used to support hydride-transfer pathways. For example, Toste and co-workers found that oxidation of (±)-methyl 2-hydroxy-2-(2-phenyl-cyclopropyl)acetate gave the corresponding ketone, thus ruling out a mechanism involving a carbinol radical.[5f]

A few previous reports have suggested that bases can promote vanadium-mediated alcohol oxidations. Ragauskas and Jiang studied the aerobic oxidation of activated benzylic and allylic alcohols with $[V^{IV}(O)(acac)_2]$ (acac = acetylacetonate) as a catalyst in the presence of 1,4-diazabicyclo[2.2.2]octane (DABCO).[5a,b] Recently, some of us reported kinetic evidence for pyridine promotion of stoichiometric oxidation of aliphatic alcohols by $[(dipic)V^{V}(O)OiPr]$ (H_2dipic = dipicolinic acid).[5a,b,21] However, the dependence of the rate on the concentration of pyridine was complex, because the base also coordinates to the catalyst. We also reported that the 8-hydroxyquinolinato complex, $[(HQ)_2V^{V}(O)OiPr]$ (**1**), catalyzes the aerobic oxidation of lignin model compounds, including benzylic, allylic, and propargylic alcohols (Scheme 1).[13] The catalytic activity of **1** in the presence of triethylamine was higher than that of several other vanadium-based catalysts.[13] Although no rate dependence on the base concentration was reported, there is no evidence that triethylamine binds to **1**, and there is no open coordination site for such binding. Therefore, we chose **1** to elucidate the precise role of the base in these vanadium-catalyzed aerobic oxidations of alcohols.

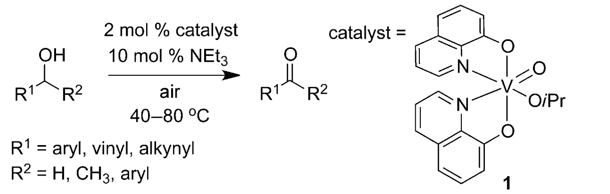

Scheme 1. Catalytic oxidation of benzylic, allylic, and propargylic alcohols by $[(HQ)_2V^{V}(O)OiPr]$ (**1**).

Herein, we present the combined results of our experimental (kinetics) and computational (density functional theory) studies on the key redox step in the catalytic oxidation of alcohols. For benzyl alcoholate complexes, we find that the external base initiates the reaction by abstracting a proton at the benzylic position. The result is an unusual base-assisted dehydrogenation, which is reminiscent of metalloenzyme pathways. The results may have important ramifications for future catalyst development because they suggest new ways to tune the activity and selectivity of vanadium catalysts for the oxidation of alcohols and other substrates.

Results

A rapid reaction takes place between $[(HQ)_2V^{V}(O)OiPr]$ (**1**) and various *para*-substituted benzyl alcohols in either THF or CH_2Cl_2 at room temperature [Eq. (1)]. Ligand exchange generates $[(HQ)_2V^{V}(O)(OCH_2C_6H_4\text{-}p\text{-}X)]$, where X is OCH_3 (**2**), H (**3**), CH_3 (**4**), F (**5**), CF_3 (**6**), or CN (**7**). Complexes **3**–**7** were characterized by ^{51}V, ^{1}H, and ^{13}C NMR spectroscopy, IR spectroscopy, and mass spectrometry; complex **2** was reported previously.[13]

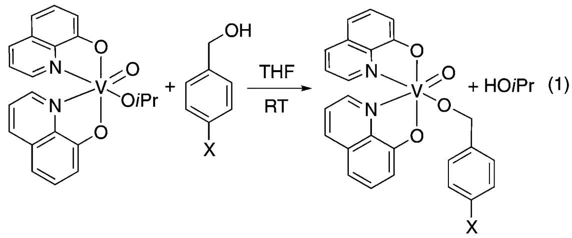

X = OCH_3 (**2**), H (**3**), CH_3 (**4**), F (**5**), CF_3 (**6**), CN (**7**)

Complexes **2**–**7** show characteristic signals in the ^{1}H NMR spectrum in the range 6.57–6.80 ppm, corresponding to the benzylic protons. These signals appear downfield from those of the free benzyl alcohols (4.57–4.77 ppm). Each complex gives one signal in the ^{51}V NMR spectrum. Differences in the ^{51}V NMR chemical shifts are slight (ranging from −473 ppm for **2**, to −477 ppm for **6**), but nevertheless correlate approximately with the electronic nature of the *para* substituent. The IR spectrum of each complex contains a peak in the narrow range 959–961 cm^{-1}, which was assigned to the V=O stretching mode.

Rate law for the intramolecular redox reaction: In the absence of added base, complex **3** is relatively stable in CD_2Cl_2 at room temperature. For example, the ^{1}H NMR spectrum showed less than 12% conversion over the course of 72 hours at 303 K. However, when NEt_3 (2 equivalents) was added to a solution of **3** in [D_4]-1,2-dichloroethane in an NMR tube at room temperature under Ar, the reaction proceeded readily and conversion was complete within 2 hours, affording benzaldehyde (0.5 equivalents, 100% yield), and benzyl alcohol (0.5 equivalents, 100% yield) [Eq. (2)].

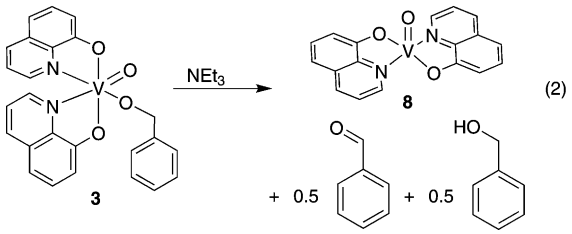

(2)

The accompanying V^{IV} product, [$(HQ)_2V^{IV}(O)$] (**8**), was isolated and identified previously.[13]

Kinetic data was obtained by monitoring, using UV/Vis spectroscopy, the intramolecular redox reaction of **3** in the presence of 24 mM NEt_3 in 1,2-dichloroethane at 303 K. The data from a typical experiment are shown in Figure 1. In the UV/Vis spectrum, there are two clean isosbestic points, at 382 and 426 nm, which persist throughout the course of the reaction, thus indicating quantitative conversion of **3** into **8** without accumulation of intermediates. The reaction is first order in **3**, with $k_{obs} = (2.62 \pm 0.10) \times 10^{-3}\ s^{-1}$, Figure 1 (inset). The linear dependence of k_{obs} on the concentration of NEt_3 is shown in Table 1 and Figure 2. The rate law is therefore also first order in NEt_3, [Eq. (3)]

$$-d[\mathbf{3}]/dt = k[NEt_3][\mathbf{3}] = k_{obs}[\mathbf{3}] \quad (3)$$

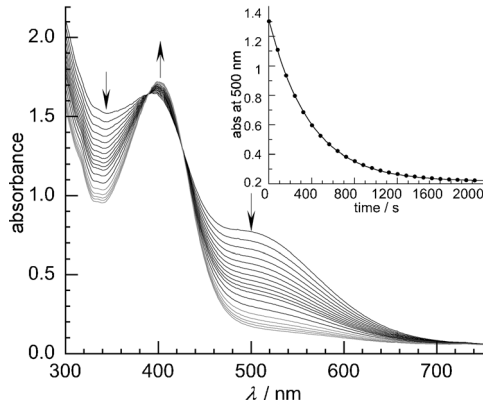

Figure 1. Time-resolved UV/Vis spectra showing the redox reaction of **3** (0.34 mM) in the presence of NEt_3 (24 mM) in 1,2-dichloroethane at 303 K under Ar. Spectra were recorded at 20 s intervals over a period of 1 h. The inset shows the evolution of the absorbance at 500 nm as a function of time, as well as the curve fit obtained using the first-order rate equation.

Table 1. Dependence of k_{obs} for the redox reaction of **3** on the concentration of NEt_3 in 1,2-dichloroethane.

T [K]	[NEt_3] [mM]	$10^3\ k_{obs}$ [s^{-1}][a]	$10^2\ k$ [$M^{-1}s^{-1}$][b]
303	12	1.57 ± 0.13	
303	24	2.62 ± 0.10	10.9 ± 0.42
303	36	4.20 ± 0.60	
303	48	5.46 ± 1.05	
303	72	8.40 ± 0.80	
293	24	1.74 ± 0.31	7.2 ± 1.3
313	24	4.35 ± 0.68	18.1 ± 2.8
323	24	5.65 ± 0.77	23.6 ± 3.2
333	24	7.98 ± 0.81	33.2 ± 3.4

[a] Each value is the average of three independent experiments. The uncertainty is the standard deviation of the average. [b] Each value is the ratio of the averaged value of k_{obs} and the concentration of NEt_3. The uncertainty is the standard deviation of k_{obs}, divided by 0.024 M.

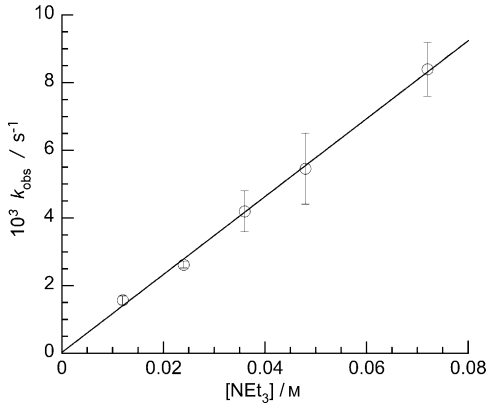

Figure 2. Dependence of the pseudo-first-order rate constants for the redox reaction of **3** on the concentration of NEt_3 in 1,2-dichloroethane at 303 K. Error bars are based on uncertainties given in Table 1.

Activation parameters: Kinetic data were collected for the redox reaction of **3** at several different temperatures, Table 1. The resulting Eyring plot, shown in Figure 3, gave $\Delta H^{\neq} = (28 \pm 4)\ kJ\,mol^{-1}$ and $\Delta S^{\neq} = (-169 \pm 4)\ J\,K^{-1}mol^{-}$.[22] The large, negative value for $\Delta S^{\neq}$ is consistent with a bimolecular reaction.

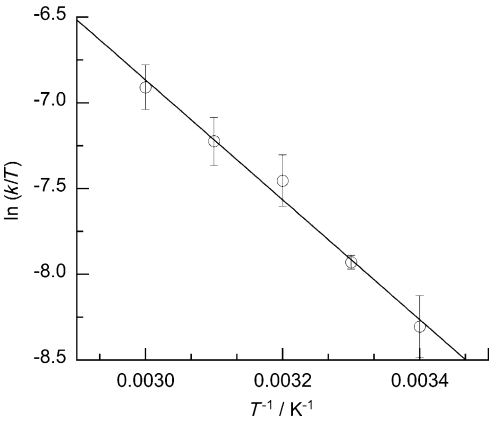

Figure 3. Eyring plot for the redox reaction of **3** in the presence of NEt_3 in 1,2-dichloroethane.

Kinetic isotope effect: The selectively deuterated complex $[(HQ)_2V^V(O)(CD_2C_5H_5)]$ ([D_2]-**3**) was prepared by the reaction of **1** with [α,α-D_2]benzyl alcohol in THF. At 303 K in 1,2-dichloroethane, the redox reaction of [D_2]-**3** ($k=(1.07\pm0.04)\times10^{-2}\,M^{-1}s^{-1}$) is an order of magnitude slower than that of unlabeled **3** ($k=(10.9\pm0.42)\times10^{-2}\,M^{-1}s^{-1}$). The kinetic isotope effect, k_H/k_D, is therefore 10.2 ± 0.6. Its magnitude confirms that it is a primary kinetic isotope effect, suggesting that cleavage of a benzylic C–H bond occurs during the rate-determining step.

***para*-Substituent effects**: To probe electronic effects on the rate of the redox reaction, the kinetics were evaluated for each member of the series $[(HQ)_2V^V(O)(OCH_2C_6H_4\text{-}p\text{-}X)]$, where X = OMe, CH_3, H, F, CF_3, and CN. The rate constants are given in Table 2, and the resulting Hammett plot, constructed using σ_p values,[23] is shown in Figure 4. The rate constants are sensitive to the identity of the *para* substituent, with electron-withdrawing substituents enhancing the reaction rate. The large positive ρ value, $+(1.34\pm0.18)$, implies that negative charge develops on the benzylic carbon atom in the transition state.

Table 2. Dependence of the rate constant for the intramolecular redox reaction of $[(HQ)_2V^V(O)OCH_2C_6H_4\text{-}p\text{-}X]$, on the nature of the *para* substituent, X.[a]

Complex	X	σ_p[b]	$10^2\,k$ [$M^{-1}\,s^{-1}$][c]
2	OCH_3	−0.27	5.46 ± 1.01
4	CH_3	−0.17	6.46 ± 0.16
3	H	0.00	10.9 ± 0.42
5	F	0.06	7.82 ± 0.46
6	CF_3	0.54	43.3 ± 1.67
7	CN	0.66	107 ± 1.68

[a] In 1,2-dichloroethane at 303 K. [b] Values from ref. [22]. [c] Each value is the average of three independent experiments. The uncertainty is the standard deviation of the average.

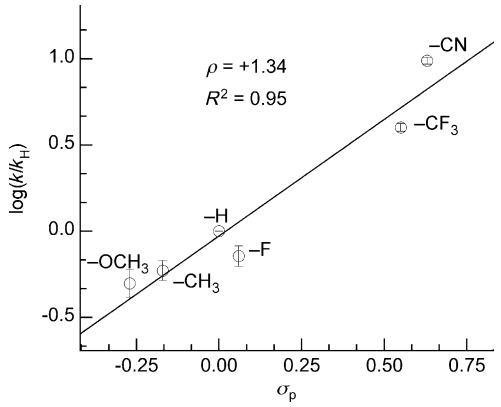

Figure 4. Hammett plot for the intramolecular redox reaction of $[(HQ)_2V^V(O)OCH_2C_6H_4\text{-}p\text{-}X]$, in 1,2-dichloroethane at 303 K.

Secondary amines: We also examined the redox reaction of **3** in the presence of various amines, HNR_2 (24 mM, 303 K). In all cases, the rate law is first order in the secondary amine. The use of the more basic amine, $HNEt_2$ ($pK_b=3.07$ in toluene), leads to a faster reaction ($k=(21.2\pm1.00)\times10^{-2}\,M^{-1}s^{-1}$) than that mediated by NEt_3 ($pK_b=3.33$; $k=(10.9\pm0.42)\times10^{-2}\,M^{-1}s^{-1}$). Interestingly, it is also more effective than the more basic, yet bulkier amine, $HNiPr_2$ ($pK_b=2.80$ in toluene; $k=(10.5\pm2.46)\times10^{-2}\,M^{-1}s^{-1}$).[24] When the even bulkier amine, $HNiBu_2$ ($pK_b=3.18$), was used, the reaction was even slower ($k=(4.38\pm1.04)\times10^{-2}\,M^{-1}s^{-1}$) than that using NEt_3. These differences in rate constants suggest that steric hindrance also plays a role in the base-assisted reaction, thus providing another means to tune the catalyst system.

Computational modeling of the reaction mechanism: DFT calculations on the singlet potential energy surface using the parent complex **3** gave a high free-energy barrier, 132 kJ mol^{-1} at 298 K, for direct intramolecular hydride transfer from the benzylic C–H bond of the alcoholate ligand to the vanadyl oxo ligand. In contrast, the calculated free-energy barrier for the intermolecular pathway is more favorable, at only 94 kJ mol^{-1}. In this mechanism, that is, base-assisted dehydrogenation (BAD), NEt_3 abstracts a proton from the benzylic position, giving coordinated benzaldehyde and, formally, a V^{III} complex. A spin crossover from singlet to the triplet state also occurs at this stage, with the latter being more stable than the former by 71 kJ mol^{-1}. The protonated base, $HNEt_3^+$, subsequently approaches the vanadyl oxo ligand and transfers a proton. This reaction is downhill, with no calculated barrier. The resulting aldehyde complex, $[(HQ)V^{III}(OH)(O{=}CHPh)]$, presumably then comproportionates with **3** to generate the V^{IV} product **8** [Eq. (3)], as previously proposed for a closely-related system.[21] Calculated transition-state geometries corresponding to intramolecular hydride transfer and the BAD mechanism are shown in Figure 5.

Computational modeling with $HNEt_2$ instead of NEt_3 revealed identical behavior, except that the free-energy barrier for transfer of the benzylic proton to $HNEt_2$ was reduced to 79 kJ mol^{-1}. This is presumably because $HNEt_2$ also forms a hydrogen bond with the oxygen atom of a hydroxyquinolinato ligand, resulting in a much closer approach (V–N) to the active site than for NEt_3, Figure 5c. Computational attempts to locate a concerted mechanism, in which a proton is transferred to the oxo ligand while the benzylic carbon atom is being deprotonated, were unsuccessful; these attempts led mostly to collapse to stepwise transition states, although one such attempt indicated a highly unfavorable process with a barrier greater than 188 kJ mol^{-1}.

A computational Hammett study was also performed to investigate *para*-substituent effects for both intra- and intermolecular reaction mechanisms. Complexes **2–6** were investigated, as was the complex with NO_2 as the *para* substituent. For intramolecular hydride transfer, the correlation between σ_p and the calculated rate constants is weak ($R^2=0.22$), although the correlation is consistent with slightly faster reactions for ligands with more electron-withdrawing *para* substituents, $\rho=+(0.26\pm0.22)$ (see the Supporting In-

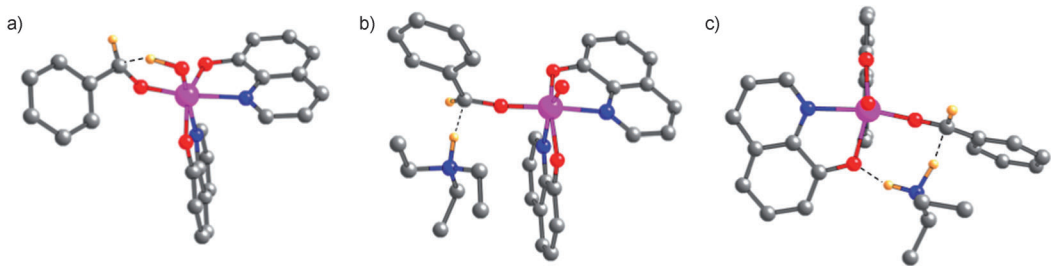

Figure 5. Calculated transition states in the redox reaction of **3**: a) intramolecular hydride transfer to the vanadyl oxo ligand, and b) and c) base-assisted dehydrogenation by NEt_3 and $HNEt_2$, respectively. For b), the distances Et_3N–H and C_{benzyl}···H are 1.17 and 1.59 Å, respectively. Most hydrogen atoms have been omitted for clarity. Color scheme: V = magenta, N = blue, C = gray, O = red, H = orange.

formation). For the mechanism based on an intermolecular BAD, the correlation between σ_p and the calculated rate constant is very good ($R^2 = 0.98$) and the effect is much stronger: $\rho = +(2.86 \pm 0.19)$. Thus computations and experiment follow the same trend, with much greater rate acceleration occurring for electron-poor benzyl alcoholate ligands.

Discussion

Most metal-mediated alcohol oxidations that involve Brønsted bases as co-catalysts operate through a fundamentally different mechanism than the one described in this study. Bases have proven to be important in both Cu-[6b] and Pd-mediated[25] alcohol oxidations, where they serve to deprotonate coordinated alcohols at the OH group, thereby generating alkoxide complexes as intermediates prior to the redox step. Detailed mechanistic studies by Sigman et al. showed the dual role of bases in Pd-catalyzed aerobic oxidation of secondary alcohols, both in coordinating themselves to the metal and in deprotonating the coordinated alcohol.[26]

For our vanadium catalyst, the base plays an unusually direct role in the redox step, that is, abstracting a proton from the α position of the alcoholate ligand (Scheme 2a). Calculations predict a free-energy barrier for NEt_3-assisted deprotonation of **3** that is 38 kJ mol^{-1} lower than for direct hydride transfer to the oxo ligand. Extracting the enthalpic and entropic components of the free-energy barriers reveals a higher enthalpic cost for intramolecular hydride transfer: $\Delta H^{\neq}$ is lower by 49 kJ mol^{-1} for intermolecular base-assisted dehydrogenation (BAD). However, the bimolecular nature of BAD also makes $\Delta S^{\neq}$ more negative, by 37 J K^{-1} mol^{-1}. Overall, the calculated activation free energy for the latter reaction is in reasonable agreement with the experimental value.

Based on these findings, we now propose an explanation for the complex rate-dependence of alcohol oxidation by [(dipic)V^V(O)(OR)] on pyridine concentration,[21] Scheme 2b. One pyridine molecule occupies the open coordination site, while a second molecule abstracts a proton from the α-position of the vanadium-bound alcoholate ligand. The rate of alcohol oxidation is significantly enhanced by

a) NEt_3-assisted alcohol dehydrogenation catalyzed by [$(HQ)_2$V(O)($OCH_2C_6H_4X$)]

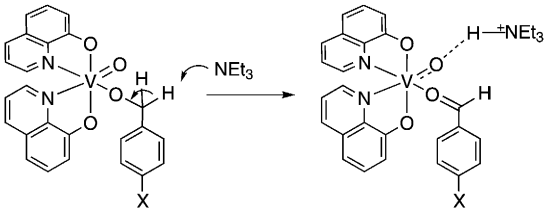

b) pyridine-assisted alcohol dehydrogenation catalyzed by [(dipic)V(O)O*i*Pr]

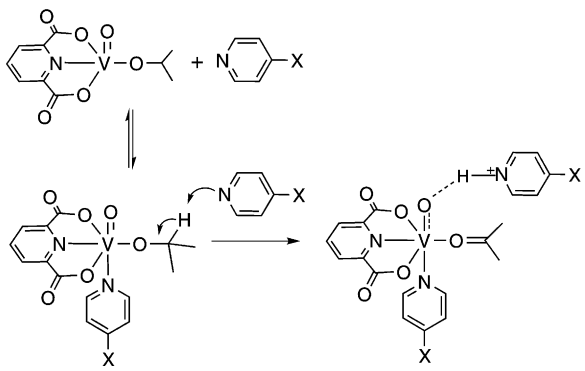

Scheme 2. Comparison of key steps in base-assisted dehydrogenation for two different [LV(O)OR] complexes, a) without, and b) with an open coordination site.

more basic substituted pyridines ($\rho = -2.5$), consistent with their role in this deprotonation step.

The proposed BAD mechanism for [$(HQ)_2$V(O)(OR)] is also supported by the agreement between the large positive experimental and calculated Hammett parameters for *para*-substituted benzyl alcohols. In contrast, most prior Hammett studies of benzylic alcohol oxidations involving metal-based oxidants report negative ρ values.[27] For example, in the oxidation of benzylic alcohols by either [$RuCl_2(PPh_3)_3$]/TEMPO[28] or [(neocuproine)Pd($OAc)_2$],[29] the ρ value was determined to be −0.58 in each case, signifying a buildup of positive charge on the benzylic carbon atom in the transition state owing to rate-limiting β-hydride elimination. When a high-valent iron–oxo complex was used to oxidize *para*-substituted benzyl alcohols, the reaction rate was not greatly influenced by the nature of the *para* substituent.[30] Poor corre-

lations with conventional Hammett σ and σ^+ values are usually attributed to radical character at the benzylic position in the transition state.[30b] For the vanadium-mediated alcohol oxidation reaction studied herein, plotting the rate as a function of σ values revealed no correlation, which is inconsistent with the potential involvement of benzyl radicals.[31]

Few reported alcohol oxidation reactions mediated by transition-metal complexes exhibit positive ρ values, and none are strongly positive. Sigman and Jensen reported a negligible ρ value (+0.03) in the $Pd(OAc)_2$-catalyzed aerobic oxidation of benzyl alcohols.[32] Recently, Guzei and coworkers observed the oxidation of primary and secondary benzylic alcohols by a tetrametallic ruthenium-oxo-hydroxo-hydride complex.[27] Whereas the Hammett correlation for the oxidation of secondary alcohols suggested negative charge buildup on the benzylic carbon atom ($\rho = +0.22$), primary alcohols displayed the opposite trend ($\rho = -0.45$).[27]

The base-assisted dehydrogenation pathway reported here resembles that of certain enzymatic oxidations, for which crystallographic and biochemical analyses suggest that the rate is highly dependent on the ability of specific catalytic residues near the active site to act as proton acceptors.[33] For example, the mechanism proposed for benzylamine oxidation by bovine serum amine oxidase involves proton abstraction by an active-site base (aspartate),[34] affording a carbanion intermediate with partial delocalization of the negative charge into the aromatic ring of the substrate. A similar mechanism involving aspartate was proposed for the oxidation of benzyl alcohols and amines by methylamine dehydrogenase, which showed an increase in rate with electron-withdrawing *para* substituents.[34–35] The reported ρ value, +1.47, is very similar to the value measured here.

Finally, DuBois and Bullock and co-workers recently demonstrated the ability of pendant bases in the second coordination sphere of nickel complexes to facilitate proton transfer,[36] reminiscent of the proton conduction channels in the active sites of hydrogenase enzymes. Pendant amines promote H_2 activation by acting as proton relays, lowering the energy barrier of the transfer of protons to and from the catalytically active metal site.[36a] DuBois, Kubiak and coworkers have shown that these complexes can be used as catalysts for the electrochemical oxidation of formate.[37] Electrochemical and spectroscopic studies suggested rate-determining proton transfer to a pendant amine ligand of the Ni–formate complex, thus avoiding direct hydride transfer to the metal center. This β-deprotonation is a multi-site proton-coupled electron transfer (MS-PCET) process. Similar to the base-assisted dehydrogenation pathway postulated herein, it involves the initial movement of a proton and two electrons to two separate sites.[38]

Conclusion

Experimental and computational studies concur that the mechanism of alcohol oxidation catalyzed by **1** likely involves a bimolecular reaction between vanadium alcoholate complexes such as **3** and an external base. The redox process involves deprotonation of the benzylic position by NEt_3 in the rate-determining step, followed by the transfer of the proton from $HNEt_3^+$ to the vanadyl oxo ligand. Thus the overall intramolecular redox reaction is in fact intermolecular, and is mediated by a redox-inactive co-catalyst. Compared to most transition-metal-catalyzed alcohol oxidations, this mechanism is highly unusual. It results in a nonradical, two-electron pathway resembling those proposed for certain metalloenzyme-catalyzed oxidations.[34–35] These mechanistic insights indicate that highly active and selective catalytic oxidation processes may be designed using first-row transition-metal catalysts in conjunction with either external bases as co-catalysts, or ligands with appropriately positioned pendant bases to serve as proton shuttles.

Experimental Section

General considerations: Unless specified otherwise, all manipulations were carried out under a dry argon atmosphere using standard glove-box and Schlenk techniques. Deuterated solvents were purchased from Cambridge Isotope Laboratories and dried over CaH_2. Anhydrous acetonitrile, CH_2Cl_2, THF, and diethyl ether were obtained from Fisher Scientific and were used as received. 1,2-Dichloroethane and NEt_3 were dried over CaH_2. In addition, dichloroethane was stored over 4 Å molecular sieves. ^1H, ^{13}C, and ^{51}V NMR spectra were recorded at room temperature on Bruker AV400 and AV500 spectrometers as well as a Varian VNMRS 600 spectrometer. Chemical shifts (δ) were referenced either internally to the residual solvent signal or externally to $VOCl_3$ (0 ppm). IR spectra were recorded on a Varian 1000 FT-IR Scimitar Series instrument. Complexes **1** and **2** were prepared as previously reported.[13] HR-MS spectra were recorded on a Micromass QTOF2 Quadrupole/Time-of-Flight Tandem mass spectrometer in the UCSB Mass Spectrometry Facility.

Synthesis of $[(HQ)_2V^V(O)(OCH_2C_6H_5)]$ (3): Benzyl alcohol (466 mg, 4.31 mmol) and $[(HQ)_2VO(OiPr)]$ (163 mg, 0.394 mmol) were dissolved in THF (2 mL). The reaction mixture was allowed to stand at room temperature for 20 min, then the solvent was removed under vacuum. The dark red residue was dissolved in THF (1 mL), and diethyl ether (10 mL) and pentane (3 mL) were added. Cooling the mixture to −20 °C overnight resulted in the formation of a dark red precipitate. After decanting the supernatant, the solid was washed with diethyl ether (2×2 mL) and dried under vacuum. Yield: 158 mg (87 %); ^1H NMR (400 MHz, CD_2Cl_2): $\delta = 8.59$ (d, 1H, $J(H,H) = 4.4$ H; HQ), 8.43 (d, 1H, $J(H,H) = 3.6$ Hz; HQ), 8.14 (d, 1H, $J(H,H) = 8.0$ Hz; HQ), 8.04 (d, 1H, $J(H,H) = 8.0$ Hz; HQ), 7.60–7.53 (m, 2H; HQ), 7.37–7.13 (m, 11H; HQ), 6.80 (d, 1H, $J(H,H) = 13.6$ Hz; V-OC*H*H), 6.65 ppm (d, 1H, $J(H,H) = 13.6$ Hz; V-OCH*H*); $^{13}C\{^1H\}$ NMR (100 MHz, CD_2Cl_2): $\delta = 164.8$, 163.5, 146.7, 146.3, 144.5, 142.9, 141.8, 141.7, 139.9, 139.0, 137.9, 130.5, 130.4, 129.8, 129.3, 128.7, 127.9, 127.6, 122.7, 122.6, 118.4, 115.4, 111.9, 110.6, 90.1 ppm; ^{51}V NMR (105 MHz, CD_2Cl_2): $\delta = -473$ ppm (s); IR: $\nu = 961$ cm^{-1} (V=O); HRMS (ESI/TOF): m/z calcd for $C_{25}H_{19}N_2O_4V + Na^+$: 485.0682 $[M+Na]^+$; found: 485.0661.

Complexes **4**–**7** were prepared following similar procedures to that described above for **3**.

$[(HQ)_2V^V(O)(OCH_2C_6H_4$-*p*-$CH_3)]$ (4): Yield: 59.7 mg (92 %); ^1H NMR (400 MHz, CD_2Cl_2): $\delta = 8.58$ (br s, 1H; HQ), 8.42 (br s, 1H; HQ), 8.15 (d, 1H, $J(H,H) = 8.0$ Hz; HQ), 8.05 (d, 1H, $J(H,H) = 8.4$ Hz; HQ), 7.60–7.53 (m, 2H; HQ), 7.28–7.07 (m, 10H; HQ), 6.75 (d, 1H, $J(H,H) = 13.6$ Hz; V-OC*H*H), 6.59 (d, 1H, $J(H,H) = 13.6$ Hz; V-OCH*H*), 2.30 ppm (s, 3H, C*H*$_3$); $^{13}C\{^1H\}$ NMR (100 MHz, CD_2Cl_2): $\delta = 164.7$, 163.4, 146.5, 146.1, 139.8, 138.8, 138.5, 137.7, 137.6, 130.4, 130.3, 129.6, 129.5, 129.3, 129.1, 127.7, 127.4, 122.5, 122.4, 118.1, 115.2, 111.7, 110.4, 105.4, 90.2, 21.3 ppm;

^{51}V NMR (105 MHz, CD_2Cl_2): $\delta = -474$ ppm (s); IR (thin film): $\nu =$ 960 cm^{-1} (V=O); HRMS (ESI/TOF): *m/z* calcd for $C_{26}H_{21}N_2O_4V+Na^+$: 499.0839 $[M+Na]^+$; found: 499.0812.

[$(HQ)_2V^V(O)(OCH_2C_6H_4$-*p*-F)] (5): Yield: 46 mg (82%); ^{1}H NMR (400 MHz, CD_2Cl_2): $\delta = 8.58$ (d, 1H, J(H,H) = 4.4 Hz; HQ), 8.42 (d, 1H, J(H,H) = 4.0 Hz; HQ), 8.15 (d, 1H, J(H,H) = 8.4 Hz; HQ), 8.05 (d, 1H, J(H,H) = 8.4 Hz; HQ), 7.60–7.53 (m, 2H; HQ), 7.35–7.11 (m, 10H; HQ), 6.96 (t, 2H; aryl), 6.72 (d, 1H, J(H,H) = 13.6 Hz; V-OC*H*H), 6.57 ppm (d, 1H, J(H,H) = 13.6 Hz; V-OCH*H*); ^{13}C{^{1}H} NMR (100 MHz, CD_2Cl_2): $\delta = 164.6$, 163.7, 163.3 (d, ^1J(C,F) = 200 Hz), 161.3 (d, ^1J(C,F) = 200 Hz), 146.5, 146.1, 141.6, 139.7, 138.9, 137.8, 137.5, 130.4, 130.3, 129.6, 129.4, 129.3, 129.1, 122.5, 122.4, 118.3, 115.4, 115.3, 115.2, 111.7, 110.3, 88.9 ppm; ^{51}V NMR (105 MHz, CD_2Cl_2): $\delta = -474$ ppm (s); IR (thin film): $\nu = 960$ cm^{-1} (V=O); HRMS (ESI/TOF): *m/z* calcd for $C_{25}H_{18}FN_2O_4V+Na^+$: 503.0588 $[M+Na]^+$; found: 503.0562.

[$(HQ)_2VO(OCH_2C_6H_4$-*p*-CF_3)] (6): Yield: 45 mg (61%); ^{1}H NMR (400 MHz, CD_2Cl_2): $\delta = 8.58$ (d, 1H, J(H,H) = 4.4 Hz; HQ), 8.42 (d, 1H, J(H,H) = 4.0 Hz; HQ), 8.15 (d, 1H, J(H,H) = 8.4 Hz; HQ), 8.05 (d, 1H, J(H,H) = 8.4 Hz; HQ), 7.60–7.53 (m, 2H; HQ), 7.35–7.11 (m, 10H; HQ), 6.96 (t, 2H; aryl), 6.72 (d, 1H, J(H,H) = 13.6 Hz; V-OC*H*H), 6.57 ppm (d, 1H, J(H,H) = 13.6 Hz; V-OCH*H*); ^{13}C{^{1}H} NMR (150 MHz, CD_2Cl_2): $\delta = 164.2$, 162.6, 146.2, 145.6, 145.4, 141.2, 139.3, 138.5, 137.4, 130.6, 130.0, 129.9, 129.8 (q, ^1J(C,F) = 32 Hz), 128.7, 126.7, 126.0, 125.22, 124.98 (q, ^1J(C,F) = 3.45 Hz), 124.4 (q, ^1J(C,F) = 272 Hz), 122.1, 122.0, 118.1, 114.9, 111.3, 109.9, 87.5 ppm; ^{51}V NMR (105 MHz, CD_2Cl_2): $\delta = -477$ ppm (s); IR (thin film): $\nu = 960$ cm^{-1} (V=O); HRMS (ESI/TOF): *m/z* calcd for $C_{26}H_{18}F_3N_2O_4V+Na^+$: 553.0556 $[M+Na]^+$; found: 553.0530.

$(HQ)_2V^V(O)(OCH_2C_6H_4$-*p*-CN) (7): Yield: 64.8 mg (95%); ^{1}H NMR (400 MHz, CD_2Cl_2): $\delta = 8.58$ (d, 1H, J(H,H) = 4.5 Hz; HQ), 8.42 (d, 1H, J(H,H) = 4.5 Hz; HQ), 8.15 (d, 1H, J(H,H) = 8.0 Hz; HQ), 8.07 (d, 1H, J(H,H) = 8.0 Hz; HQ), 7.60–7.53 (m, 2H; HQ), 7.41 (d, 2H; HQ), 7.34–7.11 (m, 2H; HQ), 6.73 (d, 1H, J(H,H) = 14.5 Hz; V-OC*H*H), 6.61 ppm (d, 1H, J(H,H) = 14.5 Hz; V-OCH*H*); ^{13}C{^{1}H} NMR (125 MHz, CD_2Cl_2): $\delta = 164.6$, 163.3, 147.4, 146.7, 146.2, 141.7, 139.7, 139.0, 137.9, 132.7, 132.4, 130.5, 130.4, 129.6, 129.2, 127.5, 127.4, 122.6, 122.5, 119.4, 118.7, 115.5, 111.8, 111.2, 110.3, 87.6 ppm; ^{51}V NMR (105 MHz, CD_2Cl_2): $\delta = -476$ ppm (s); IR (thin film): $\nu = 959$ cm^{-1} (V=O); HRMS (ESI/TOF): *m/z* calcd for $C_{26}H_{18}N_3O_4V+Na^+$: 510.0635 $[M+Na]^+$; found: 510.0610.

Synthesis of [α,α-D_2]-benzyl alcohol (9): The synthesis of [α,α-D_2]-benzyl alcohol was carried out according to a reported literature procedure.[39] Yield: 88.6 mg (38%); ^{1}H NMR (400 MHz, $CDCl_3$): $\delta = 7.37$ (m, 4H), 7.33–7.28 ppm (m, 1H).

Synthesis of [$(HQ)_2V^V(O)(OCD_2C_6H_5)$] ([$D_2$]-3): The procedure was similar to that used for the synthesis of unlabeled **3**. Yield: 98 mg (97%); ^{1}H NMR (500 MHz, CD_2Cl_2): $\delta = 8.59$ (d, 1H, J(H,H) = 4.5 Hz; HQ), 8.43 (d, 1H, J(H,H) = 4.5 Hz; HQ), 8.15 (d, 1H, J(H,H) = 8.0 Hz; HQ), 8.05 (d, 1H, J(H,H) = 8.5 Hz; HQ), 7.59–7.53 (m, 2H; HQ), 7.36–7.13 ppm (m, 12H; HQ); ^{13}C{^{1}H} NMR (100 MHz, CD_2Cl_2): $\delta = 164.7$, 163.4, 146.5, 146.1, 141.6, 141.5, 139.8, 138.9, 137.8, 130.4, 130.3, 129.6, 129.1, 128.9, 128.6, 127.8, 127.6, 127.3, 122.5, 122.4, 118.2, 115.2, 111.7, 110.4, 89.2 ppm; ^{51}V NMR (105 MHz, CD_2Cl_2): $\delta = -479.4$ ppm (s); IR (thin film): $\nu = 960$ cm^{-1} (V=O); HRMS (ESI/TOF): *m/z* calcd for $C_{25}H_{17}D_2N_2O_4V+Na^+$: 488.0886 $[M+Na]^+$; found: 487.0791.

Kinetics experiments: All experiments were carried out under Ar in 1,2-dichloroethane, using square quartz cuvettes (path length, 1 cm) sealed with Teflon septum caps. In a typical experiment, NEt_3 was added by syringe to a thermally equilibrated cuvette containing 3 mL of a solution of the vanadium complex (0.3–0.4 mM). The concentration of NEt_3 was varied in the range 12–72 mM to evaluate its reaction order, then held constant at 24 mM for all other measurements. Reactions were initiated by the addition of NEt_3. The absorbance at 500 nm was recorded as a function of time, using an Agilent 8453 UV/Vis spectrophotometer equipped with a Peltier thermostatted cell holder for complexes **2**–**5**. For complexes **6** and **7**, experiments were performed on a Shimadzu UV-2401PC spectrometer equipped with a TCC-240 A thermoelectrically temperature-controlled cell holder. First-order rate constants were calculated by non-linear least-squares fitting (with uniform data weighting) of the integrated first-order rate equation [Eq (4)]; A_∞ is the final absorbance at completion of the reaction, A_0 is the initial absorbance, A_t is the absorbance measured at time t, and k_{obs} is the pseudo-first-order rate constant.

$$A_t = A_\infty + (A_0 - A_\infty)\exp(-k_{obs}t) \quad (4)$$

Computational methods: Mechanisms were investigated at the M06/6–311++(d,p) level of theory. Density functional theory (DFT) simulations employed the Gaussian 09 package.[40] The M06 functional[41] was used in conjunction with the extended Pople basis set, 6–311++G(d,p) and an ultrafine integration grid.[42]

All quoted energies are free energies calculated at 298.15 K and 1 atm, using unscaled vibrational frequencies. Stationary points were characterized as minima or transition states via calculation of the energy Hessian and observation of the correct number of imaginary frequencies (zero or one, respectively). All geometry optimizations were performed without symmetry restraints. A restricted or unrestricted Kohn–Sham formalism was used for closed- and open-shell species, respectively. Both singlet and triplet energy surfaces were explored. The singlets were consistently lower in energy than the triplets by at least 84 kJ mol^{-1}; consequently, only singlet energies are reported here unless otherwise indicated.

Acknowledgements

This work was supported by the NSF through the Center for Enabling New Technologies through Catalysis (CENTC). In addition, B.N.W acknowledges support from the ConvEne IGERT Program (NSF-DGE 0801627). S.K.H. thanks the LANL Institute for Multiscale Materials Studies for support. Portions of this work were performed using the Central Facilities of the Materials Research Laboratory at UC Santa Barbara, supported by the MRSEC Program of the NSF under Award No. DMR 1121053 and a member of the NSF-funded Materials Research Facilities Network (www.mrfn.org).

[1] M. Hudlick, *Oxidations in Organic Chemistry*, American Chemical Society, Washington, DC, **1990**.

[2] a) R. Aldea, H. Alper, *J. Org. Chem.* **1995**, *60*, 8365–8366; b) T. F. Blackburn, J. Schwartz, *J. Chem. Soc. Chem. Commun.* **1977**, 157–158; c) E. M. Ferreira, B. M. Stoltz, *J. Am. Chem. Soc.* **2001**, *123*, 7725–7726; d) M. J. Schultz, R. S. Adler, W. Zierkiewicz, T. Privalov, M. S. Sigman, *J. Am. Chem. Soc.* **2005**, *127*, 8499–8507; e) S. S. Stahl, *Angew. Chem.* **2004**, *116*, 3480—3501; *Angew. Chem. Int. Ed.* **2004**, *43*, 3400–3420.

[3] a) L. Liu, M. Yu, B. B. Wayland, X. Fu, *Chem. Commun.* **2010**, *46*, 6353–6355; b) H. Mimoun, M. M. Perez-Machirant, I. Sérée de Roch, *J. Am. Chem. Soc.* **1978**, *100*, 5437–5444; c) B. de Bruin, P. H. M. Budzelaar, *Angew. Chem.* **2004**, *116*, 4236–4251; *Angew. Chem. Int. Ed.* **2004**, *43*, 4142–4157; d) C. Tejel, M. A. Ciriano, *Top. Organomet. Chem.* **2007**, *22*, 97–124.

[4] a) C. Bilgrien, S. Davis, R. S. Drago, *J. Am. Chem. Soc.* **1987**, *109*, 3786–3787; b) I. E. Markó, P. R. Giles, M. Tsukazaki, I. Chellé-Regnaut, C. J. Urch, S. M. Brown, *J. Am. Chem. Soc.* **1997**, *119*, 12661–12662; c) E. Takezawa, S. Sakaguchi, Y. Ishii, *Org. Lett.* **1999**, *1*, 713.

[5] a) N. Jiang, A. J. Ragauskas, *Tetrahedron Lett.* **2007**, *48*, 273–276; b) N. Jiang, A. J. Ragauskas, *J. Org. Chem.* **2007**, *72*, 7030–7033; c) Y. Maeda, N. Kakiuchi, S. Matsumura, T. Nishimura, T. Kawamura, S. Uemura, *J. Org. Chem.* **2002**, *67*, 6718–6724; d) Y. Maeda, N. Kakiuchi, S. Matsumura, T. Nishimura, S. Uemura, *Tetrahedron Lett.* **2001**, *42*, 8877–8879; e) C. Ohde, C. Limberg, *Chem. Eur. J.* **2010**, *16*, 6892–6899; f) A. Radosevich, C. Musich, F. D. Toste, *J. Am. Chem. Soc.* **2005**, *127*, 1090–1091; g) S. Velusamy, T. Punniyamurthy, *Org. Lett.* **2004**, *6*, 217–219.

[6] a) P. Chaudhuri, M. Hess, U. Florke, K. Wieghardt, *Angew. Chem.* **1998**, *110*, 2340–2343; *Angew. Chem. Int. Ed.* **1998**, *37*, 2217–2220; b) P. Gamez, I. W. C. E. Arends, J. Reedijk, R. A. Sheldon, *Chem. Commun.* **2003**, 2414–2415; c) N. Jiang, A. J. Ragauskas, *J. Org.*

Chem. **2006**, *71*, 7087–7090; d) C. Michel, P. Belanzoni, P. Gamez, J. Reedijk, E. J. Baerends, *Inorg. Chem.* **2009**, *48*, 11909–11920.
[7] a) P. J. Chirik, K. Wieghardt, *Science* **2010**, *327*, 794; b) W. I. Dzik, J. I. van der Vlugt, J. N. H. Reek, B. de Bruin, *Angew. Chem.* **2011**, *123*, 3416–3418; *Angew. Chem. Int. Ed.* **2011**, *50*, 3356–3358.
[8] V. Lyaskovskyy, B. de Bruin, *ACS Catal.* **2012**, *2*, 270–279.
[9] a) M. Costas, M. P. Mehn, M. P. Jensen, L. Que Jr., *Chem. Rev.* **2004**, *104*, 939–986; b) R. A. Himes, K. D. Karlin, *Curr. Opin. Chem. Biol.* **2009**, *13*, 119–131; c) A. M. Kirillov, M. N. Kopylovich, M. V. Kirillova, M. Haukka, M. F. C. Guedes da Silva, A. J. L. Pombeiro, *Angew. Chem.* **2005**, *117*, 4419—4423; *Angew. Chem. Int. Ed.* **2005**, *44*, 4345—4349; d) R. Mas-Ballesté, M. Costas, T. van den Berg, L. Que Jr., *Chem. Eur. J.* **2006**, *12*, 7489–7500; e) M. Merkyx, D. A. Kopp, M. H. Sazinsky, J. L. Blazyk, J. Müller, S. J. Lippard, *Angew. Chem.* **2001**, *113*, 2860–2888; *Angew. Chem. Int. Ed.* **2001**, *40*, 2782–2807; f) L. Que Jr., W. B. Tollman, *Nature* **2008**, *455*, 333–340.
[10] a) B. Askevold, H. W. Roesky, S. Schneider, *ChemCatChem* **2012**, *4*, 307–320; b) H. Grützmacher, *Angew. Chem.* **2008**, *120*, 1838–1842; *Angew. Chem. Int. Ed.* **2008**, *47*, 1814–1818.
[11] S. J. Lippard, J. M. Berg, *Principles of Bioinorganic Chemistry*, University Science Books, Mill Valley, CA, **1994**.
[12] a) W. I. Dzik, X. P. Zhang, B. de Bruin, *Inorg. Chem.* **2011**, *50*, 9896–9903; b) A. M. Tondreau, C. C. Hojilla Atienza, K. J. Weller, S. A. Nye, K. M. Lewis, J. G. P. Delis, P. J. Chirik, *Science* **2012**, *335*, 567–570.
[13] S. K. Hanson, R. Wu, L. A. Silks, *Org. Lett.* **2011**, *13*, 1908–1911.
[14] a) A. Blanc, F. D. Toste, *Angew. Chem.* **2006**, *118*, 2150–2153; *Angew. Chem. Int. Ed.* **2006**, *45*, 2096–2099; b) V. D. Pawar, S. Bettigeri, S. S. Weng, J. Q. Kao, C. T. Chen, *J. Am. Chem. Soc.* **2006**, *128*, 6308–6309; c) S. Weng, M. Shen, J. Kao, Y. S. Munot, C. Chen, *Proc. Natl. Acad. Sci. USA* **2006**, *103*, 3522.
[15] a) I. K. Meier, J. Schwartz, *J. Am. Chem. Soc.* **1989**, *111*, 3069–3070; b) I. K. Meier, J. Schwartz, *J. Org. Chem.* **1990**, *55*, 5619–5624.
[16] T. Hirao, Y. Ohshiro, *Tetrahedron Lett.* **1990**, *31*, 3917–3918.
[17] T. Hirao, T. Fujii, Y. Ohshiro, *Tetrahedron Lett.* **1994**, *35*, 8005–8008.
[18] a) B. Sedai, C. Diaz-Urrutia, R. T. Baker, R. Wu, L. A. Silks, S. K. Hanson, *ACS Catal.* **2011**, *1*, 794–804; b) S. Son, F. D. Toste, *Angew. Chem.* **2010**, *122*, 3879–3882; *Angew. Chem. Int. Ed.* **2010**, *49*, 3791–3794.
[19] J. Rocek, D. E. Aylward, *J. Am. Chem. Soc.* **1975**, *97*, 5452.
[20] a) J. S. Littler, W. A. Waters, *J. Chem. Soc.* **1959**, 4046–4052; b) J. S. Littler, W. A. Waters, *J. Chem. Soc.* **1959**, 1299–1305; c) J. S. Littler, W. A. Waters, *J. Chem. Soc.* **1960**, 2767–2772.
[21] S. K. Hanson, T. R. Baker, J. C. Gordon, B. L. Scott, L. A. Silks, D. L. Thorn, *J. Am. Chem. Soc.* **2010**, *132*, 17804–17816.
[22] P. M. S. Morse, M. D. Wilson, S. R. Girolami, *Organometallics* **1994**, *13*, 1646–1655.
[23] D. H. McDaniel, H. C. Brown, *J. Org. Chem.* **1958**, *23*, 420–427.
[24] J. J. Christensen, R. M. Izatt, D. P. Wrathall, L. D. Hansen, *J. Chem. Soc. A* **1969**, 1212–1223.
[25] J.-E. Bäckvall, *In Modern Oxidation Methods*, Wiley-VCH, Weinheim, Germany, **2004**.
[26] a) D. R. Jensen, J. S. Pugsley, M. S. Sigman, *J. Am. Chem. Soc.* **2001**, *123*, 7475–7476; b) S. K. Mandal, M. S. Sigman, *J. Org. Chem.* **2003**, *68*, 7535–7537; c) J. A. Mueller, D. R. Jensen, M. S. Sigman, *J. Am. Chem. Soc.* **2002**, *124*, 8202–8203; d) J. A. Mueller, M. S. Sigman, *J. Am. Chem. Soc.* **2003**, *125*, 7005–7013.
[27] C. S. Yi, T. N. Zeczycki, I. A. Guzei, *Organometallics* **2006**, *25*, 1047–1051.
[28] A. Dijksman, A. Marino-Gonzalez, A. Mairata i Payeras, I. W. C. E. Arends, R. A. Sheldon, *J. Am. Chem. Soc.* **2001**, *123*, 6826–6833.
[29] G.-J. ten Brink, I. W. C. E. Arends, M. Hoogenraad, G. Verspui, R. A. Sheldon, *Adv. Synth. Catal.* **2003**, *345*, 497–505.
[30] a) M. Newcomb, Z. Pan, *Inorg. Chem.* **2007**, *46*, 6767–6774; b) N. Y. Oh, Y. Suh, M. J. Parks, M. S. Seo, J. Kim, W. Nam, *Angew. Chem.* **2005**, *117*, 4307—4311.
[31] X. Creary, M. E. Mehrsheikh-Mohammadi, S. McDonald, *J. Org. Chem.* **1987**, *52*, 3254–3263.
[32] M. S. Sigman, D. R. Jensen, *Acc. Chem. Res.* **2006**, *39*, 221–229.
[33] G. J. Bartlett, C. T. Porter, N. Borkakoti, J. M. Thornton, *J. Mol. Biol.* **2002**, *324*, 105–121.
[34] C. Hartmann, J. P. Klinman, *Biochemistry* **1991**, *30*, 4605–4611.
[35] V. L. Davidson, L. H. Jones, M. E. Graichen, *Biochemistry* **1992**, *31*, 3385–3390.
[36] a) D. L. DuBois, M. R. Bullock, *Eur. J. Inorg. Chem.* **2011**, 1017–1027; b) M. O'Hagan, W. J. Shaw, S. Raugei, S. Chen, J. Y. Yang, U. R. Kilgore, D. L. DuBois, M. R. Bullock, *J. Am. Chem. Soc.* **2011**, *133*, 14301–14312.
[37] B. R. Galan, J. Schoffel, J. C. Linehan, C. Seu, A. M. Appel, J. A. S. Roberts, M. L. Helm, U. J. Kilgore, J. Y. Yang, D. L. DuBois, C. P. Kubiak, *J. Am. Chem. Soc.* **2011**, *133*, 12767–12779.
[38] C. S. Seu, A. M. Appel, M. D. Doud, D. L. DuBois, C. P. Kubiak, *Energy Environ. Sci.* **2012**, *5*, 6480–6490.
[39] A. D. N. Vaz, M. J. Coon, *Biochemistry* **1994**, *33*, 6442–6449.
[40] Gaussian 09, Revision A. 1, M. J. Frisch, G. W. Trucks, H. B. Schlegel, G. E. Scuseria, M. A. Robb, J. R. Cheeseman, G. Scalmani, V. Barone, B. Mennucci, G. A. Petersson, H. Nakatsuji, M. Caricato, X. Li, H. P. Hratchian, A. F. Izmaylov, J. Bloino, G. Zheng, J. L. Sonnenberg, M. Hada, M. Ehara, K. Toyota, R. Fukuda, J. Hasegawa, M. Ishida, T. Nakajima, Y. Honda, O. Kitao, H. Nakai, T. Vreven, J. Montgomery, J. A., J. E. Peralta, F. Ogliaro, M. Bearpark, J. J. Heyd, E. Brothers, K. N. Kudin, V. N. Staroverov, R. Kobayashi, J. Normand, K. Raghavachari, A. Rendell, J. C. Burant, S. S. Iyengar, J. Tomasi, M. Cossi, N. Rega, N. J. Millam, M. Klene, J. E. Knox, J. B. Cross, V. Bakken, C. Adamo, J. Jaramillo, R. Gomperts, R. E. Stratmann, O. Yazyev, A. J. Austin, R. Cammi, C. Pomelli, J. W. Ochterski, R. L. Martin, K. Morokuma, V. G. Zakrzewski, G. A. Voth, P. Salvador, J. J. Dannenberg, S. Dapprich, A. D. Daniels, Ö. Farkas, J. B. Foresman, J. V. Ortiz, J. Cioslowski, D. J. Fox, Gaussian, Inc., Wallingford, CT, **2009**.
[41] Y. Zhao, D. G. Truhlar, *Acc. Chem. Res.* **2008**, *41*, 157.
[42] a) P. J. Hay, *J. Chem. Phys.* **1977**, *66*, 4377; b) R. Krishnan, J. S. Binkley, R. Seeger, J. A. Pople, *J. Chem. Phys.* **1980**, *72*, 650; c) A. D. McLean, G. S. Chandler, *J. Chem. Phys.* **1980**, *72*, 5639; d) A. J. H. Wachters, *J. Chem. Phys.* **1970**, *52*, 1033.

Received: July 13, 2012
Published online: October 18, 2012

